Infrared Study of the Surface Properties of HTB-Type Al−, Cr−, Fe−Hydroxyfluorides

Alexandre Vimont,[†] Jean-Claude Lavalley,[†] Loïc Francke,[‡] Alain Demourgues,[‡] Alain Tressaud,[‡] and Marco Daturi*[,†]

Laboratoire de Catalyse et Spectrochimie, UMR 6506 CNRS-ENSICaen, 6, bd Maréchal Juin, F-14050 Caen Cedex, France, and Institut de Chimie de la Matière Condensée de Bordeaux, CNRS, 87, av Docteur A. Schweitzer, F-33608 Pessac Cedex, France

Received: August 21, 2003; In Final Form: December 23, 2003

The surface properties of iron, chromium, and aluminum fluorides in their hexagonal tungsten bronze (HTB) form have been investigated by infrared spectroscopy. The presence of hydroxyls is clearly observed. H/D exchange experiments with different deuterated probe molecules having various molecular sizes show that they are localized inside of the channels of the structure. The ν(OH) bands in the infrared spectra of these materials are downward shifted compared to those of corresponding metal oxides, whereas the δ(OH) in-plane bending mode presents an unusual high wavenumber. These spectral features are compared to those observed on zeolites, for which hydroxyl environment and bridged conformation are similar. HTB compounds exhibit both strong Lewis and Brønsted acid sites. The use of two basic probes with a different size (pyridine and ammonia) allows one to localize and to quantify these two kinds of acidity. Brønsted acidity is related to the presence of hydroxy groups into the microporous channels and to chemisorbed HF, whereas Lewis acidity is due to defect sites both on the outer surface of crystallites and in the channels. The strength of acid sites is unambiguously found stronger than that reported for Al, Cr, and Fe oxides. This result is discussed taking into account the electronegativity of fluorine but also the bridged conformation of OH groups, as in the case of zeolites.

Introduction

Fluorinated and hydroxyfluoride compounds are interesting materials because they are good catalysts for many important industrial reactions as aromatic alkylation[1,2] or halogen exchange in CFCs and HFCs.[3] However, the knowledge of their surface properties, necessary to understand the key parameters governing their catalytic activities, is relatively limited with respect to the parent oxides. In fact it is well-known that fluorination or chlorination of the surface of numerous oxides affects their catalytic activity,[1−4] but the influence of halogenation on the surface properties has been clearly investigated only for alumina,[5] for which it has been observed that fluorination increases the surface acidity and modifies the nature of the hydroxy groups.[5,6] The results appear to depend on the fluorination method used and the fluorine content. To avoid such experimental features, in the present work, we focus on well crystallized fluorinated materials. The crystalline structure of these compounds is related to that of hexagonal tungsten bronzes (HTB), like that of M_xWO_3 bronzes. In particular, it exhibits one-dimensional channels of about 3−4 Å diameter, free from cations, in which water molecules occupy well-defined crystallographic sites.[7,8] Preliminary results on the characterization of HTB fluoride samples used in the present study have shown the presence of hydroxy groups, as evidenced by infrared spectroscopy.[9] Such hydroxyls can play an important role in catalysis and it is therefore important to localize them and to measure their acidity. To determine whether the hydroxy groups are on the outer surface or in the channels, experiments based on H/D exchange using deuterated probe molecules such as tertiobutanol-OD, D_2O, and even D_2 have been performed. As for the acidity determination, two basic probe molecules, pyridine and ammonia, have been used. These probes allow us to distinguish between Brønsted and Lewis acidity and to quantify them. The ammonia molecule ($\sigma = 0.12$ nm^2) is smaller than pyridine ($\sigma = 0.28$ nm^2) and equivalent to water ($\sigma = 0.109$ nm^2). Therefore, NH_3 can better diffuse inside the channels of the HTB structure and therefore reaches a higher proportion of acidic sites than in the case of pyridine. The results are compared to those related for the parent metal oxides, e.g., Fe_2O_3, Cr_2O_3, and Al_2O_3. Up to now, no surface characterization by infrared spectroscopy has been reported for FeF_3, whereas those concerning aluminum[10,11] and chromium compounds[12] are not numerous and have not taken into account the accessibility factor.

Experimental Section

As described in a previous paper,[13] the different samples were prepared by various routes of synthesis: either by thermal degradation of the ammonium metal fluoride ($(NH_4)_3MF_6$), by dehydration of the trihydrated metal fluoride ($MF_3 \cdot 3H_2O$), or by fluorination of the hydroxide $M(OH)_3$ under anhydrous HF in the case of chromium fluoride. HTB (β) $AlF_{3-x}(OH)_x$ was also obtained by thermal dehydration of $AlF_3 \cdot 3H_2O$. The starting compound $AlF_3 \cdot 3H_2O$ was prepared from an alcoholic aluminum(III) nitrate solution, which favored the precipitation of $AlF_3 \cdot 3H_2O$ which is less soluble in ethanol than in water. Aluminum(III) nitrate nanohydrate was dissolved in a large amount of (ethanol:water) = (7:3) solution. A stoichiometric aqueous solution of HF was slowly added. The precipitate was filtered, washed with a large amount of water and ethanol, and dried overnight at 363 K. HTB−AlF_3 was then obtained by

* To whom correspondence should be addressed. E-mail: daturi@ismra.fr. Phone: +33-231452730. Fax: +33-231452822.
[†] Laboratoire de Catalyse et Spectrochimie.
[‡] Institut de Chimie de la Matière Condensée de Bordeaux.

10.1021/jp036496z CCC: $27.50
Published on Web 02/13/2004

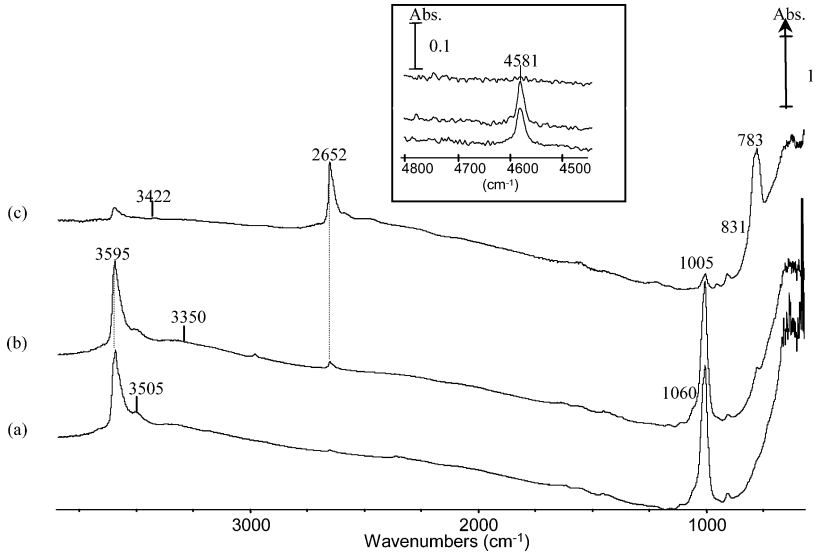

Figure 1. Infrared spectra of $FeF_{3-x}(OH)_x$, after calcination at 473 K under vacuum (10^{-4} Pa) (spectrum a), then introduction of the equilibrium pressure $P_e = 666$ Pa of tertiobutanol-OD at room temperature and evacuation under vacuum at 373 K (spectrum b); then introduction of $P_e = 1333$ Pa of D_2O at 373 K and evacuation under vacuum at 473 K (spectrum c). Inset: infrared range of the $\nu+\delta$(OH) combination band.

dehydration of $AlF_3 \cdot 3H_2O$ under vacuum at 493 K during 5 h followed by a thermal treatment under argon atmosphere during 14 h at 723 K.

HTB$-FeF_{3-x}(OH)_x \cdot \delta H_2O$ and HTB$-Fe_{0.8}Cr_{0.2}F_{3-x}(OH)_x \cdot \delta H_2O$ were prepared from their homologous trihydrated fluorides, under "self-generated" atmosphere at 493 K during 16 h. The starting materials $MF_3 \cdot 3H_2O$ was obtained from an alcoholic M(III) nitrate solution, as described above.

Due to the tendency of chromium salts to form pyrochlore hydroxyfluoride phases, a Cr^{III}-based HTB phase could not successfully been synthesized by thermal dehydration of $CrF_3 \cdot 3H_2O$. Therefore the chosen route was the thermal decomposition of $(NH_4)_3CrF_6$ under a "self-generated" atmosphere. Moreover, to avoid the presence of any ammonium group which would generate basic properties in the final material, another route was developed. $Cr(OH)_3 \cdot 3H_2O$ reactant was prepared by precipitation from an aqueous chromium(III) nitrate solution. Chromium(III) nitrate nanohydrate was dissolved in a large amount of water. A stoichiometric amount of a 30% NH_4OH aqueous solution was then slowly added. The green precipitate was filtered, washed with a large amount of water, and dried overnight at 363 K. The chromium(III) trihydrated hydroxide was then dehydrated at 373 K during 14 h under an argon flow and then fluorinated under an anhydrous HF flow at 323 K during 8 h. The as-prepared amorphous solid was then placed in a platinum tube sealed under argon atmosphere and heated at 498 K during 16 h. In this latter process, the ammonium content remained smaller than in the case of the thermal decomposition of $(NH_4)_3CrF_6$. In a previous study,[9] F^- and OH^- amounts in the different samples have been evaluated: in the case of Al compounds, the estimated formula is $AlF_{2.20}(OH)_{0.80} \cdot 0.29H_2O$ for $AlF_3 \cdot 3H_2O$ route.

Powders were first characterized by X-ray diffraction and chemical analysis.[9,13] The HTB structural features of these phases were clearly confirmed by X-ray[9] and neutron diffraction experiments; no spurious phases or compounds were detected. The thermal decomposition was also investigated.[13] For FTIR spectroscopy, samples were pressed (10^7-10^9 Pa) into self-supported disks (2 cm^2 area, 7−20 mg cm^{-2}). They were placed in a quartz cell equipped with KBr windows. A movable quartz sample holder permits the pellet to be adjusted in the infrared beam for spectra acquisition and to displace it into a furnace at the top of the cell for thermal treatments. Spectra were recorded at room temperature after quenching the sample from the thermal treatment temperature. The cell was connected to a vacuum line for evacuation and calcination steps ($P_{residual} = 10^{-3}-10^{-4}$ Pa). Addition of accurately known increments of probe molecules in the cell was possible via a calibrated volume connected to a pressure gauge and a control of the probe pressure by a gauge.

A Nicolet Magna 750 IR spectrometer equipped by a DTGS detector and an XT-KBr beam splitter was used for the acquisition of spectra recorded in the 500−5600 cm^{-1} range.

Samples were activated by calcination under vacuum (10^{-4} Pa) by heating (1 K/min) up to a limit temperature nonexceeding that of sample decomposition (i.e., fluorine departure). According to the thermogravimetric analysis coupled with mass spectrometer,[13] these temperatures are 613 K for $AlF_{3-x}(OH)_x$ prepared by decomposition of trihydrated fluoride, 473 K for $FeF_{3-x}(OH)_x$ and $Fe_{0.8}Cr_{0.2}F_{3-x}(OH)_x$, and 373 K for $CrF_{3-x}(OH)_x$. For instance in the case of $AlF_{3-x}(OH)_x$ prepared by decomposition of trihydrated fluoride, the OH concentration determined by chemical analysis[13] is high and the x value is equal to 0.8.

Results

Hydroxy Groups: Nature and Accessibility Determination. *$FeF_{3-x}(OH)_x$ HTB and $Fe_{0.8}Cr_{0.2}F_{3-x}(OH)_x$ HTB.* $FeF_{3-x}(OH)_x$ and $Fe_{0.8}Cr_{0.2}F_{3-x}(OH)_x$ HTB samples show strong absorption bands in the 3200−4000 cm^{-1} ν(OH) range (Figures 1 and 2, spectrum a). A strong and slightly asymmetric band is observed at 3595 cm^{-1}, and weaker features at 3505 cm^{-1} ($FeF_{3-x}(OH)_x$) and 3520 cm^{-1} ($Fe_{0.8}Cr_{0.2}F_{3-x}(OH)_x$) are also detected.

In both spectra, a broad absorption band is detected between 2800 and 3500 cm^{-1} and another at 1640 cm^{-1}, characterizing traces of water strongly bonded to the surface.

IR spectra b in Figures 1 and 2 are recorded after tertiobutanol OD treatment (see caption for experimental details). After introduction of tertiobutanol OD, no significative decrease of ν(OH) band intensities is observed; consequently, only a very weak band at 2652 cm^{-1} is detected in the 2700−2600 cm^{-1} ν(OD) stretching range . Therefore, it is concluded that the amount of OH groups accessible to tertiobutanol is negligible.

By contrast, after D_2O exchange (spectrum c, Figures 1 and 2, see caption for experimental details), ν(OH) band intensities

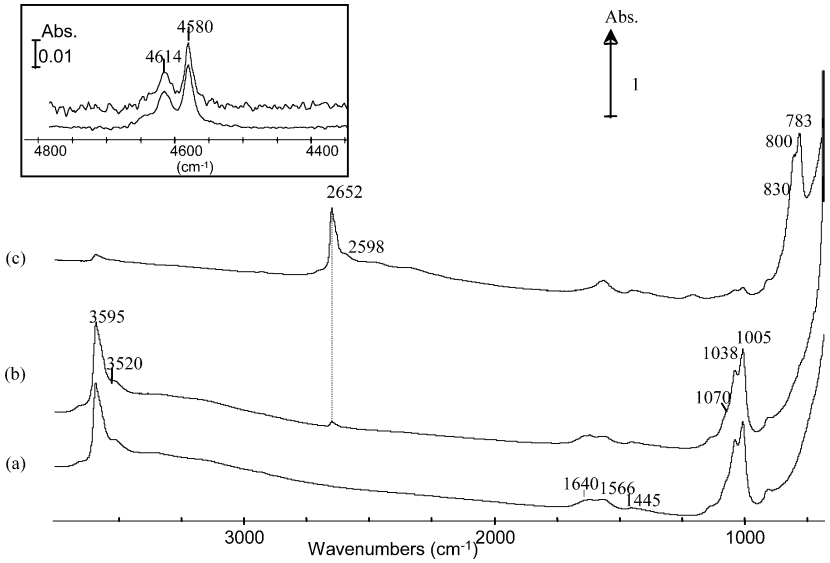

Figure 2. Infrared spectra of $Fe_{0.8}Cr_{0.2}F_{3-x}(OH)_x$, after calcination at 473 K under vacuum (10^{-4} Pa) (spectrum a), then introduction of $P_e = 666$ Pa of tertiobutanol-OD at room temperature and evacuation under vacuum at 373 K (spectrum b); then introduction of $P_e = 1333$ Pa of D_2O at 373 K and evacuation under vacuum at 473 K (spectrum c). Inset: infrared range of the $\nu+\delta$(OH) combination band.

TABLE 1: Recapitulative Table of OH(D) Bands of Hydroxyls Observed on the Spectra of the HTB Compounds after Activation

compound	hydroxyl bands			assignments
	$\nu_{(OH)}/\nu_{(OD)}$ (cm^{-1})	$\delta_{(OH)}/\delta_{(OD)}$ (cm^{-1})	$(\nu+\delta)_{OH}$ (cm^{-1})	
$Fe_{0.8}Cr_{0.2}F_{3-x}(OH)_x$	3595/2652	1005/783	4580	bridged OH group (Fe site)
	3595/2652	1038/800	4614	bridged OH (closed to Cr site)
		1070/830		
$FeF_{3-x}(OH)_x$	3595/2652	1005/783	4581/3422	bridged OH group
		1060/831		
$CrF_{3-x}(OH)_x$	~3600 (awaited)	1070	4650	bridged OH group
$AlF_{3-x}(OH)_x$	3665/2701	1128/879	4772	bridged Al−OH group

strongly decrease. Simultaneously, ν(OD) bands are clearly observed at 2652 and 2582 cm^{-1} ($FeF_{3-x}(OH)_x$) and at 2652 and 2598 cm^{-1} ($Fe_{0.8}Cr_{0.2}F_{3-x}(OH)_x$), corresponding (according to the ratio ν(OH)/ν(OD) equal to 1.355) to OD groups having replaced hydroxy groups initially observed at 3595 and 3505 cm^{-1} and 3595 and 3520 cm^{-1}, respectively. For the sake of clarity, OH and OD band wavenumbers have been summarized in Table 1. Intensity measurements of ν(OH) bands before and after exchange show that almost all of the hydroxy groups are accessible to D_2O since at least 85% of them have been exchanged.

Before H/D exchange, the $FeF_{3-x}(OH)_x$ spectrum displays a sharp IR band at 1005 cm^{-1} with a shoulder at 1060 cm^{-1}. In the case of the $Fe_{0.8}Cr_{0.2}F_{3-x}(OH)_x$ material, three bands are observed at 1005, 1038, and 1070 cm^{-1} (shoulder). They are not sensitive to deuterated tertiobutanol treatment, whereas after D_2O treatment, they disappear while new bands are observed at 783 and 831 cm^{-1} for FeF_3 and at 783, 800, and 830 cm^{-1} for $Fe_{0.8}Cr_{0.2}F_{3-x}(OH)_x$. Therefore, due to this sensitivity to deuterium exchange, these bands are not due to Fe−F vibration modes, fundamentals, or overtones but to hydroxy groups deformation modes. The isotopic effect 1060/831 and 1005/783 cm^{-1} equal to 1.28 suggests an in-plane deformation mode (δ(OH)) character as it will be discussed below.

The NIR region of the unexchanged sample spectra gives information about the vibrational modes associated with the above-mentioned bands: the $FeF_{3-x}(OH)_x$ spectrum shows a band at 4581 cm^{-1} assigned to a combination band involving those at 3595 and 1005 cm^{-1}. Such a combination band confirms that the 1005 cm^{-1} feature has a δ(OH) character. The anharmonicity coefficient is equal to 19 cm^{-1}. After D_2O treatment, a weak band is observed at 3422 cm^{-1} (Figure 1c) and corresponds to the $(\nu+\delta)$OD combination band. Note that, in the case of the $Fe_{0.8}Cr_{0.2}F_{3-x}(OH)_x$ spectrum, two bands are observed between 4650 and 4500 cm^{-1}. Comparison with $FeF_{3-x}(OH)_x$ strongly suggests that the supplementary band at 4614 cm-1 is certainly associated to the supplementary δ(OH) band observed at 1038 cm^{-1}. Taking into account the anharmonicity coefficient of about 20 cm^{-1}, we deduce that the 4614 cm^{-1} band corresponds to the combination 3595+1038 cm^{-1}. This shows that the δ(OH) and the combination $(\nu+\delta)$OH ranges are more sensitive than the ν(OH) range to the heterogeneity of the OH-groups.

$CrF_{3-x}(OH)_x$ HTB. Figure 3, spectrum a, represents the infrared spectrum of the $CrF_{3-x}(OH)_x$ sample after outgassing at 373 K during 24 h. The low signal/noise ratio is due to the necessity of using a high quantity of material (30 mg) to prepare a self-supported disk. This high quantity partly explains why the sample is not transparent to the IR beam in the 3600−2500 cm^{-1} range. Moreover, after evacuation at low temperature, ammonia and water remain strongly absorbing in this range. The presence of a strong band at 1610 cm^{-1} characterizes water retained onto the sample. In addition to a band at 5239 cm^{-1} due to the $(\nu+\delta)H_2O$ combination band, a band is detected at 4650 cm^{-1}, associated to the $(\nu+\delta)$OH combination. Taking into account the strong δ(OH) band detected at 1070 cm^{-1} and considering an anharmonic coefficient closed to 20 cm^{-1} (as observed in the case of $FeF_{3-x}(OH)_x$) the frequency of the ν-(OH) band at about 3600 cm^{-1} is deduced.

A strong band at 1427 cm^{-1} is also detected, typical of the $\delta_a(NH_4)$ vibration of ammonium ions, probably formed on Brønsted acid sites by ammonia introduced during the synthesis

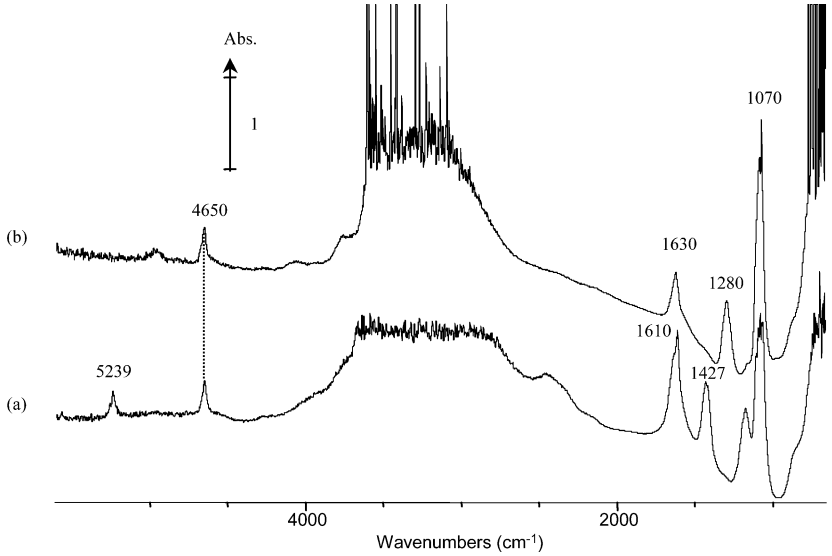

Figure 3. Infrared spectra of $CrF_{3-x}(OH)_x$, after calcination at 373 K under vacuum (10^{-4} Pa) (spectrum a) and after calcination at 473 K under vacuum (spectrum b).

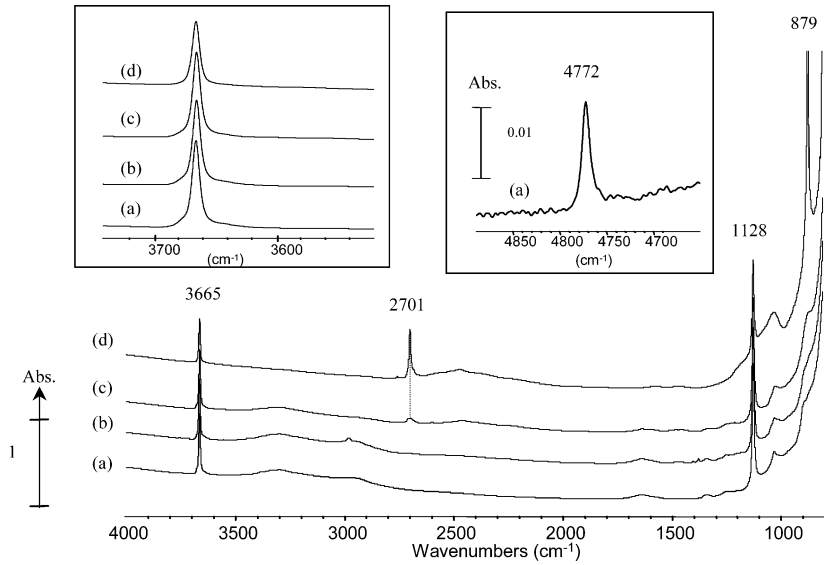

Figure 4. Infrared spectra of $AlF_{3-x}(OH)_x$, after calcination at 613 K under vacuum (10^{-4} Pa) (spectrum a), then introduction of $P_e = 666$ Pa of tertiobutanol-OD at room temperature and evacuation under vacuum at 373 K (spectrum b); then introduction of $P_e = 1333$ Pa of D_2O at 373 K and evacuation under vacuum at 613 K (spectrum c), after heating at 573 K under $P_e = 1.33 \times 10^5$ Pa of D_2 (spectrum d). Left and right insets: zoom of the ν(OH) and $\nu+\delta$(OH) regions, respectively.

step of the material. Outgassing $CrF_{3-x}(OH)_x$ in more severe conditions (473 K) permits the elimination of the bands at 5239 and 1427 cm^{-1} (Figure 3b), showing that water and ammonia, respectively, have been desorbed from the surface. However, new bands at 1280 and 1630 cm^{-1} are observed and assigned to coordinated ammonia on Lewis acid sites created at the expense of ammonium species. Therefore, it appears that residual ammonia from $CrF_{3-x}(OH)_x$ synthesis is chemisorbed as ammonium ions in the presence of Brønsted acid sites and converted to ammonia coordinated onto Lewis sites upon thermal treatment. D_2O and terbutanol OD do not produce any isotopic exchange of the free hydroxy groups, characterized by bands at 4650 and 1070 cm^{-1}, suggesting that micropores are certainly blocked by ammonia present onto the surface.

$AlF_{3-x}(OH)_x$ HTB. The IR spectrum of $AlF_{3-x}(OH)_x$ outgassed at 613 K (Figure 4a) shows a well defined ν(OH) band at 3665 cm^{-1}. In the NIR range, a narrow band is observed at 4772 cm^{-1}. These bands are not sensitive to tertiobutanol OD exposure (Figure 4b). The occurrence of a very weak ν(OD) band at 2701 cm^{-1} after D_2O exchange (Figure 4c) shows that the OH groups are slightly accessible to heavy water molecules. By contrast, after D_2 treatment at 553 K (Figure 4d), the intensity of the ν(OD) band at 2701 cm^{-1} is significant, whereas that of bands at 3665 and 4772 cm^{-1} has decreased. It can be deduced that about half of the hydroxy groups are exchangeable by D_2. In Figure 4a, a sharp band is situated at 1128 cm^{-1} and shifts to 879 cm^{-1} upon H/D exchange. These bands are assigned to the δ(OH)/δ(OD) vibration mode of OH groups giving rise to the stretching frequency at 3665/2701 cm^{-1}. In agreement, the ($\nu+\delta$)OH combination mode at 4772 cm^{-1} (3665+1128 cm^{-1}, with an anharmonicity coefficient of 21 cm^{-1}) is clearly observed. The position of the different hydroxyl bands for all of the studied compounds is summarized in Table 1.

Acidity Measurements by Basic Probe Molecules: Pyridine and NH_3. *Pyridine Adsorption.* Acidity of materials has been first probed by pyridine adsorption. This probe molecule clearly permits the nature of the acidic sites to be identified. Infrared spectra of the different samples after introduction of

TABLE 2: Significative Coordinated Pyridine and Pyridinium Ion Vibrations on the Different HTB Compounds

	sensitive modes of coordinated pyridine on Lewis acid sites		pyridinium
compounds	ν_{8a} (cm^{-1})	ν_{19b} (cm^{-1})	ν_{19b} at 1545 cm^{-1}
$FeF_{3-x}(OH)_x$	1609 (r.t.)	1447 (r.t.)	yes (r.t.)
	1613 (473 K)	1449 (473 K)	no (373 K)
$Fe_{0.8}Cr_{0.2}F_{3-x}(OH)_x$	1609 (r.t.)	1447 (r.t.)	no
	1613 (473 K)	1449 (473 K)	
$CrF_{3-x}(OH)_x$	1612 (r.t.)	1448 (r.t.)	no
$AlF_{3-x}(OH)_x$.	1620 (r.t.)	1454 (r.t.)	no
	1627 (573 K)	1456 (573 K)	

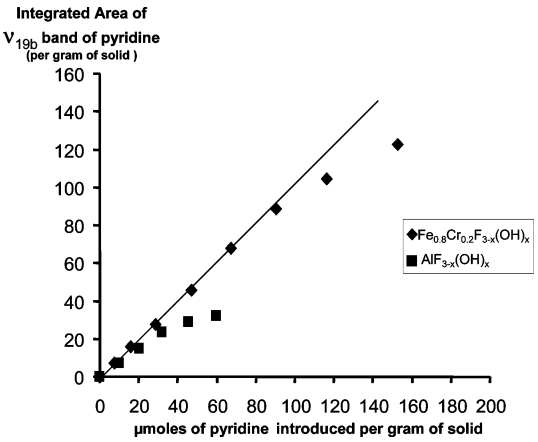

Figure 5. Integrated intensity of ν_{19b} band of coordinated pyridine at about 1450 cm^{-1} versus concentration of pyridine introduced into the cell at 423 K.

the equilibrium pressure $P_e = 133$ Pa of pyridine followed by evacuation at room temperature have been previously presented (Figure 8 in ref 9) excepted for $CrF_{3-x}(OH)_x$. The characteristic adsorbed pyridine bands in the 1400−1700 cm^{-1} range are summarized in Table 2. The formation of coordinated species on the surface is detected for all of the samples but with a low concentration in the case of $CrF_{3-x}OH_x$, because of the lower activation temperature of the sample. An additional band at 1545 cm^{-1} in the spectrum of $FeF_{3-x}(OH)_x$ indicates the formation of pyridinium species that easily desorbs after outgassing at 473 K.

For quantitative measurements, some experiments have been performed by adding successive small doses (10−20 μmol g^{-1}) of pyridine on the activated samples. In Figure 5, the variation of the integrated area of the ν_{19b} band, situated at about 1456−1447 cm^{-1}, has been reported versus the amount of pyridine introduced. A linear plot, almost identical for both compounds studied ($Fe_{0.8}Cr_{0.2}F_{3-x}(OH)_x$ and $AlF_{3-x}(OH)_x$), is initially observed suggesting that the first doses of pyridine introduced are totally chemisorbed as coordinated species. The change of the slope is well explained by the formation of physisorbed species (band at 990 cm^{-1}, not shown here). The slope of the straight line allows us to deduce the apparent extinction coefficient of the ν_{19b} band: it is close to 1.7−1.9 μmol cm^{-1}, a value similar to that reported on metal oxides.[14] After introduction of $P_e = 133$ Pa of pyridine, outgassing at room-temperature desorbs physisorbed species. From the intensity of the ν_{19b} band, the amount of pyridine coordinated after saturation can be deduced. It is about 125 μmol g^{-1} on $Fe_{0.8}Cr_{0.2}F_{3-x}(OH)_x$ and 35 μmol g^{-1} on $AlF_{3-x}(OH)_x$. Taking into account the surface area of these samples, 55 and 20 m^2/g, respectively, the number of molecules of pyridine coordinated can be estimated to 1.2−1.3 per nm^2. Such a value is in agreement with that reported for alumina activated at 573 K (1.65 per nm^2 [15]). As for $FeF_{3-x}(OH)_x$, on which pyridinium and coordinated species are formed, we deduce from the ν_{19b} band intensity a value close to 100 μmol g^{-1} for the coordinatively unsaturated sites.

Ammonia Adsorption on $FeF_{3-x}(OH)_x$ and $Fe_{0.8}Cr_{0.2}F_3$ HTB. Ammonia is often used as a probe molecule to distinguish between Brønsted and Lewis acid sites: the infrared spectrum of coordinated ammonia presents characteristic $\delta_s(NH_3)$ and $\delta_a(NH_3)$ bands at about 1200−1300 and 1620 cm^{-1}, respectively, whereas a band at about 1400−1450 cm^{-1} characterizes the $\delta_a(NH_4)$ bending mode of protonated species. H-bonded species give rise to a $\delta_s(NH_3)$ band at about 1000−1100 cm^{-1}.[16]

Ammonia has been introduced quantitatively in the IR cell at 423 K to facilitate its diffusion and to prevent the formation of weak adsorbed species. Infrared spectra of $FeF_{3-x}(OH)_x$ and $Fe_{0.8}Cr_{0.2}F_{3-x}(OH)_x$ samples during ammonia adsorption and desorption are presented in Figure 6. In the 700−1700 cm^{-1} range, spectra are similar: they show a strong band at 1425 cm^{-1} characteristic of ammonium species formation. Two other weaker features at 1612 and 1260 cm^{-1} are assigned to coordinated NH_3 species. Another band at about 840 cm^{-1} is also detected; its intensity seems to vary similarly to that at 1425 cm^{-1}. In the 4000−2800 cm^{-1} range, ammonia adsorption provokes the appearance of a complex massif between 2500 and 3400 cm^{-1}, assigned to the ν(N−H) bands of ammonia and ammonium species. The decrease in intensity of the ν(OH) bands at 3595 cm^{-1} is clearly observed and is correlated with the decrease of those at about 1000−1060 cm^{-1}, in agreement with their assignment to the δ(OH) vibrations of the same hydroxyl. After introduction of $P_e = 400$ Pa of ammonia into the cell, the intensity of the 3595 cm^{-1} has strongly decreased, becoming analogous to that observed after D_2O treatment. It shows that a large amount of hydroxy groups are accessible to NH_3 and D_2O molecules and that these groups are acidic since they give rise to ammonium species. Evacuation at 373 K and then 473 K (spectra 1g and 1h) partly eliminates ammonium species, whereas bands characterizing free hydroxy groups are not restored at all in the case of $FeF_{3-x}(OH)_x$. The same feature occurs in the case of $Fe_{0.8}Cr_{0.2}F_{3-x}(OH)_x$ when outgassing from 373 to 423 K (Figure 6, spectra 2g and 2i). By contrast, when outgassing at 473 K, a large amount of NH_4^+ species are desorbed from that sample, leading to a partial restoration of OH groups, mainly those characterized by the 1038 cm^{-1} δ(OH) band. The different behavior of the two types of hydroxy groups is confirmed when NH_3 is added: Figure 6, spectra 2a to 2g clearly evidence a preferential perturbation of OH groups characterized by the δ(OH) band at 1005 cm^{-1}. This suggests an acidity difference of the two kinds of OH groups, those characterized by the 1005 cm^{-1} band being more acidic.

On both samples, the intensity of the ammonia coordinated band at about 1260 cm^{-1} is very weak compared to that of the ammonium band at 1425 cm^{-1}, suggesting that ammonia adsorption mainly occurs under the form of ammonium species. We have plotted in Figure 7 the variation of the 1425 cm^{-1} band area versus the amount of ammonia introduced. A linear

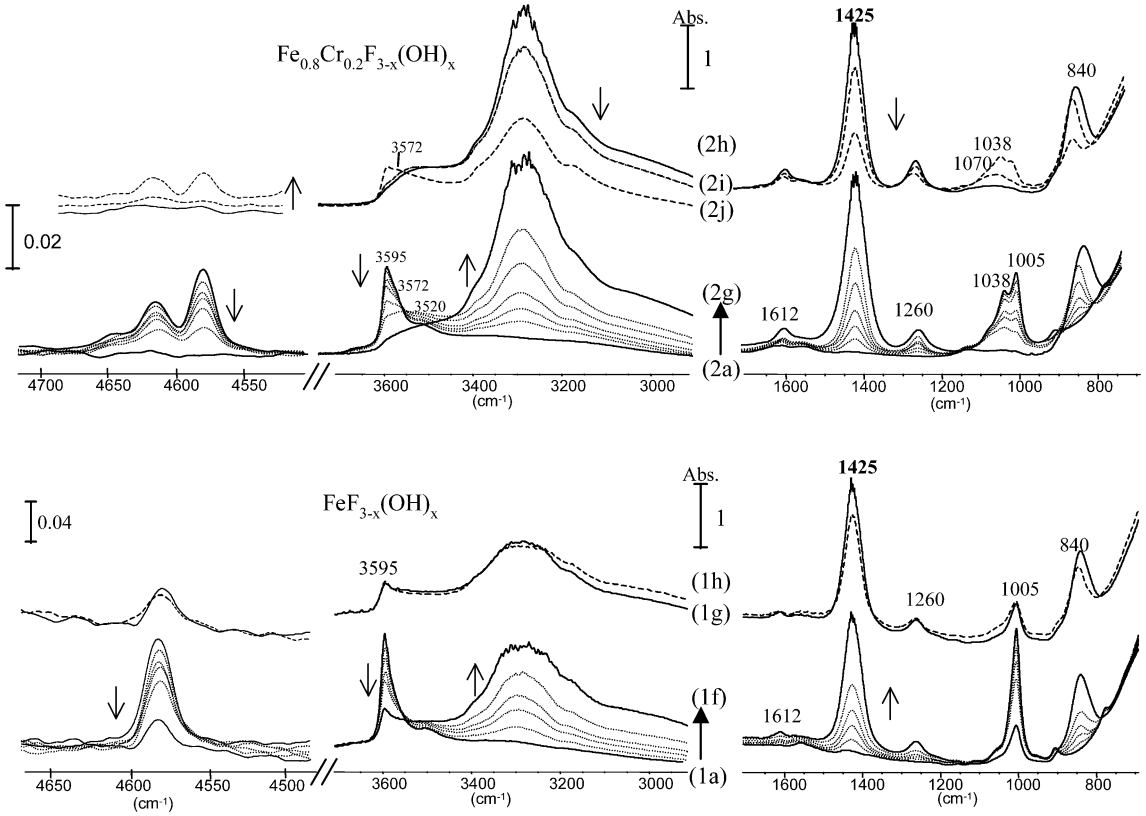

Figure 6. Infrared spectra of $FeF_{3-x}(OH)_x$ and $Fe_{0.8}Cr_{0.2}F_{3-x}(OH)_x$ during introduction of NH_3 into the IR cell and then desorption. $FeF_{3-x}(OH)_x$: spectrum 1a before NH_3 adsorption; spectra 1b−f: after introduction into the cell at 423 K of 120, 240, 360, and 750 μmol g^{-1} and then $P_e = 666$ Pa of NH_3, respectively. Spectra 1g and 1h: after evacuation under vacuum at 373 and 473 K, respectively. $Fe_{0.8}Cr_{0.2}F_{3-x}(OH)_x$: spectrum 2a before NH_3 adsorption; spectra 2b to 2g respectively after introduction into the cell at 423 K of 140, 260, 380, 630, and 920 μmol and $P_e = 666$ Pa of NH_3; spectra 2h, 2i, and 2j respectively after evacuation under vacuum at 373, 423, and 473 K.

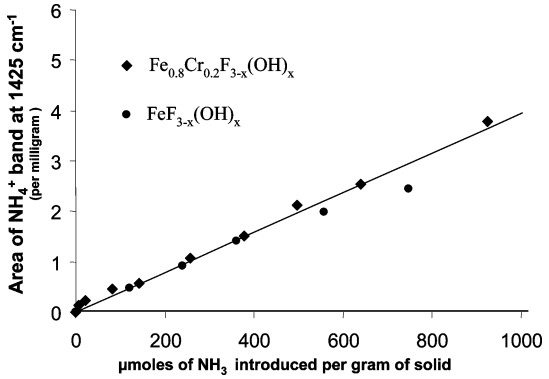

Figure 7. Integrated intensity of ammonium band ($\delta_a(NH_4)$) at 1425 cm^{-1} versus concentration of ammonia introduced into the cell at 423 K.

variation is observed. Its slope leads to an apparent extinction coefficient of about 8 μmol cm^{-1}, slightly lower than that reported on zeolites (11 μmol cm^{-1}).[17] Such a difference is well explained by the occurrence on $FeF_{3-x}(OH)_x$ and $Fe_{0.8}Cr_{0.2}F_{3-x}(OH)_x$ samples of a small amount of coordinated species. From these results, we can estimate the number of Brønsted acid sites to about 1100 and 600 μmol g^{-1} on $FeF_{3-x}(OH)_x$ and $Fe_{0.8}Cr_{0.2}F_{3-x}(OH)_x$, respectively.

To determine the nature of Brønsted acid sites involved in NH_4^+ species formation, we have studied the effect of NH_3 adsorption on the intensity of bands due to hydroxy groups. Since the $(\nu+\delta)$OH combination band is better resolved than the ν(OH) one, we have determined the variation of the combination band intensity versus the NH_3 amount introduced. Figure 8 shows a linear trend for both studied samples, showing that OH groups are well involved in the NH_4^+ species formation. However data related to desorption experiments at 373, 423, and 473 K does not fit the curve, showing that other acidic centers have also to be taken into account, as it will be discussed below.

Infrared difference spectrum of $CrF_{3-x}(OH)_x$ after introduction of ammonia into the cell is shown in Figure 9. Ammonia adsorption on $CrF_{3-x}(OH)_x$ mainly gives rise to ammonium species (band at 1440 cm^{-1}) and formation of coordinated species, in a smaller amount (band at 1284 cm^{-1}). Note that the 1440 cm^{-1} band in Figure 9 adds to that already present at the same wavenumber in the spectrum of the activated sample. The perturbation of the δ(OH) band at 1070 cm^{-1} (negative band in Figure 9) shows that ammonia protonation involves free hydroxy groups. On $AlF_{3-x}(OH)_x$, only a band at a relatively high wavenumber (1312 cm^{-1}) is detected and characterizes NH_3 species strongly coordinated on Lewis acid sites (spectrum not shown).

Discussion

IR Spectra of OH Groups. $MF_{3-x}(OH)_x$ compounds are constituted by $M^{III}(F,OH)_6$ corner sharing octahedra. The resulting framework is related to that of hexagonal tungsten bronzes. Hexagonal cavities are formed and lead to one-dimensional channels along the *c* axis with a six membered ring[7,8] (Scheme 1). The maximum diameter of these channels is 3.30 Å for $AlF_{3-x}(OH)_x$ and 3.60 Å for $FeF_{3-x}(OH)_x$.

Infrared spectra of the different HTB materials clearly show OH bands characterizing the occurrence of hydroxyls. For divided metal oxides, the origin of OH groups is due to the necessity to complete the coordinence of cations in the exposed

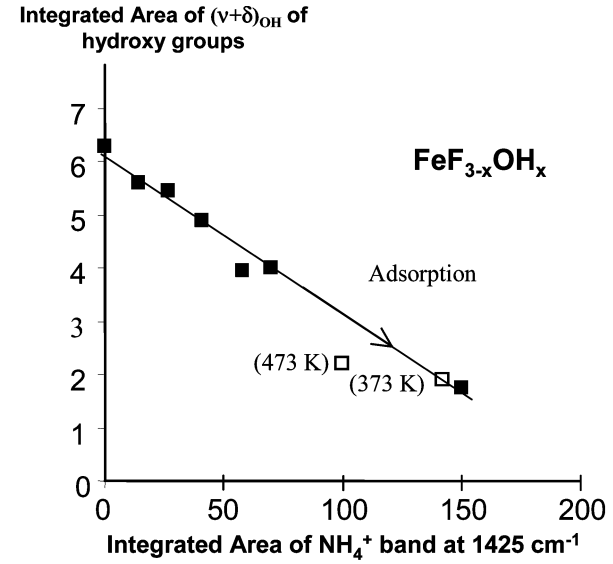

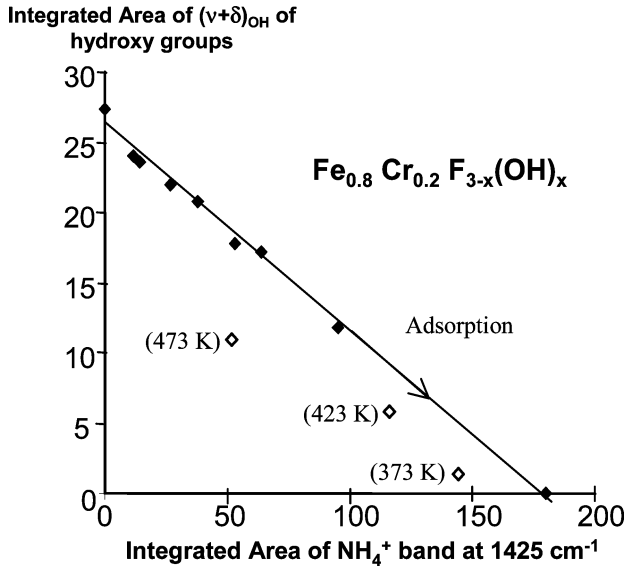

Figure 8. Variation of the area of the $\nu+\delta$(OH) combination band versus the NH_3 amount introduced into the cell and after outgassing at different temperatures (indicate on the graph).

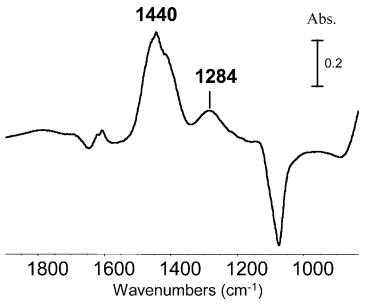

Figure 9. Infrared difference spectrum for $CrF_{3-x}(OH)_x$ after introduction into the cell of $P_e = 666$ Pa of NH_3 at 373 K (the reference spectrum is that of the activated sample).

crystallographic surface planes. For HTB fluorinated compounds, in principle no OH groups are expected. The partial substitution of OH^- groups for $F-$ anions occurs during the decomposition of hydrated precursors. From the structure of the samples, the hydroxy groups share vertexes of two octahedral cations and can be considered as type II according to their coordination number. The sharp ν(OH) band observed at 3665 cm^{-1} for $AlF_{3-x}(OH)_x$, 3595 cm^{-1} for $FeF_{3-x}(OH)_x$, and awaited at about 3600 cm^{-1} for $CrF_{3-x}(OH)_x$ is therefore assigned to these lattice hydroxy groups.

SCHEME 1: Conformation of Bridged Hydroxyls into a Truncate Fragment of the HTB Structure (left) and Representation of the Channel Aperture into the Structure (right).

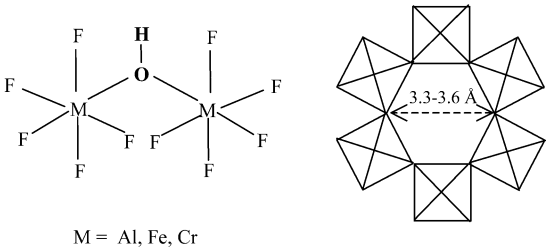

H/D exchange experiments show that the accessibility of these hydroxy groups depends on the size of the deuterated probe molecule used. In general, tertiobutanol does not have access to hydroxy groups since no isotopic exchange is observed. On the contrary, hydroxy groups are exchanged by D_2O, the $AlF_{3-x}(OH)_x$ sample excepted. In this latter case, the accessibility is very low: only D_2 partly exchanges the OH groups, in agreement with the lower channel diameter of $AlF_{3-x}(OH)_x$. We conclude that these hydroxy groups not exchanged by deuterated tertiobutanol but by D_2O or D_2 are localized into the channels of the HTB structure.

Another important point is the relative low frequency of the ν(OH) band observed in the spectra of the HTB materials: about 3595 cm^{-1} for iron and chromium HTB material, whereas OH groups are clearly pointed above 3600 cm^{-1} in the case of α- and γ-Fe_2O_3[18] and α-Cr_2O_3.[19] Furthermore, the ν(OH) band of $AlF_{3-x}(OH)_x$ HTB is observed at a lower wavenumber (3665 cm^{-1}) than those detected on alumina (between 3680 and 3800 cm^{-1}). It has been observed on zeolites having small pores (six- and eight-membered ring) such as chabbazzite and erionite, an unusual downward shift of the ν(OH) frequency of hydroxy groups compared to zeolites with larger pores.[20] This structural effect has been explained by electrostatic interactions favored by the small channel size. The channels of the HTB structure are comparable to those presented by zeolites with small pores. So, an analogous confinement effect well explains the low ν-(OH) band frequency of the hydroxyls in HTB materials. This interpretation is in agreement with the higher frequency position of the ν(OH) bands of hydroxyls on α-AlF_3 (bands at 3680 and 3702 cm^{-1}),[9] a structure for which a very small channel with a diameter lower than 0.2 nm occurs (ReO_3-type structure deriving from perovskite). However, ν(OH) bands observed on α-AlF_3 and partially fluorinated alumina are positioned also at a lower wavenumber than ν(OH) on alumina, suggesting that fluorine inductive effects can also influence the ν(OH) band position.

The in-plane bending vibrational mode of the hydroxyls is unambiguously well detected in the 1000−1200 cm^{-1} range in the HTB infrared spectra. On metal oxides, these vibrational modes are generally indirectly detected via the $(\nu+\delta)$OH combination band in the NIR range.[21] Lavalley et al. have studied the low-frequency IR spectrum range of different metal oxides.[22] They have observed that the frequency of the δ(OH) band of OH groups is often situated close to the cutoff of the samples. They have proposed to explain this phenomenon by a coupling between the δ(OH) mode and the metal−oxygen ν(M−OH) mode. The ratio δ(OH)/δ(OD) on HTB materials, deduced by H/D exchange experiments, is equal to 1.28 for $FeF_{3-x}(OH)_x$ and $AlF_{3-x}(OH)_x$. It is slightly lower than the theoretical value for a pure in plane bending mode (1.36). Such

TABLE 3: Comparative Position of the Sensitive Bands of Basic Probe Molecules Coordinated onto the Surface of Different Oxides and HTB Materials

	sensitive mode of acidic probe molecules	
compounds	ammonia $\delta_s(NH_3)$	pyridine ν_{8a}
β-FeF_3	1260 cm^{-1}	1609 cm^{-1} (r.t.) 1613 cm^{-1} (473 K)
α-Fe_2O_3[18]	1180, 1220 cm^{-1}	1608 cm^{-1}
γ-Fe_2O_3[28]		1608 cm^{-1}
β-CrF_3	1284 cm^{-1}	1612 cm^{-1} (r.t.)
α-Cr_2O_3[27]	1220 cm^{-1}	1608 cm^{-1}
β-AlF_3	1312 cm^{-1}	1620 cm^{-1} (r.t.) 1627 cm^{-1} (473 K)
γ-Al_2O_3[27]	1295 cm^{-1} 1265, 1220 cm^{-1}	1625, 1615 cm^{-1}

a difference has also been observed for silica (1.26) for which a coupling of the δ(OH) and ν(M−O) modes has been reported.[23] The existence of such a coupling likely occurs in HTB since a mass effect of the cation on the δ(OH) band position is observed: 1128 cm^{-1} for Al, 1070 cm^{-1} for Cr, and 1005 cm^{-1} for Fe homologous compounds. Another important feature is the relatively high frequency of the δ(OH) mode. For corresponding metal oxides, it is detected at lower wavenumbers: about 860−900 cm^{-1} for δ-FeOOH [24] and below 900 cm^{-1} on alumina.[25] By contrast, in zeolites, the δ(OH) mode of ≡Si−OH−Al≡ bridged hydroxy groups is often observed above 1000 cm^{-1}, whereas for unbridged isolated ≡Si−OH groups, it is detected at about 760 cm^{-1} in silica.[26] Thus, the blue shift of the δ(OH) band observed on HTB spectra could be explained again by a "structural effect" induced by a strong bridged conformation of hydroxyls in the HTB lattice (Scheme 1); moreover confinement effect may also occur. Note that, for all of the compounds studied, the ($\nu+\delta$)OH combination bands are clearly observed and perfectly fit the expected values, considering an anharmonicity coefficient of about 20 cm^{-1}. In the case of mixed iron and chromium HTB compounds, the presence of two δ(OH) bands and two corresponding ($\nu+\delta$)-OH combination bands can be explained considering that some OH groups are bridged to two Fe cations (the OH bands are then those observed for $FeF_{3-x}(OH)_x$), the others being bridged either to an Fe and Cr cation or even to two Cr cations. The δ(OH) frequency of the latter compound is higher than that observed for $FeF_{3-x}(OH)_x$. This effect can be related to the difference of chemical bond strengths mainly due to the high crystal field stabilization in the case of trivalent chromium, even if it is difficult to conclude since the bending mode is influenced by different factors.

Fluorine Effect on the Acidic Properties of HTB Materials. Acidic sites of HTB material have been probed by pyridine and ammonia. These two probes, quite basic, do not give concordant results relative to hydroxyls acidity: NH_3 generally shows that they are acidic since ammonium species are formed. By contrast, pyridine hardly affects them, even when a excess of pyridine is introduced, before evacuation (spectra not shown). This is well explained considering that hydroxy groups are situated in micropores, not accessible to pyridine.

Pyridine and ammonia adsorption on HTB materials give rise to coordinated species. The strength of the acidic sites can be estimated by the position of the ν_{8a} and $\delta_s(NH_3)$ bands in the spectrum of coordinated pyridine and ammonia, respectively.[27] The higher the position of these bands, the stronger the acidic Lewis sites are. In Table 3, we have compared band positions observed on Fe, Cr, and Al HTB materials with those reported for Al_2O_3, Fe_2O_3, and Cr_2O_3 oxides.[28−30] In all of the cases, we observe that the ν_{8a} band of coordinated pyridine on HTB compounds is located at about 3 or 4 wavenumbers higher than on the corresponding oxides. This feature expresses the stronger Lewis acidity of HTB materials. A confirmation is given by the position of the characteristic band of coordinated ammonia: a blue shift of several tens of cm^{-1} is observed for δ_s-(NH_3) referring to metal oxides: about 20 cm^{-1} for $AlF_{3-x}(OH)_x$, 40 cm^{-1} for $FeF_{3-x}(OH)_x$, and more than 50 cm^{-1} in the case of $CrF_{3-x}(OH)_x$.

H/D exchange experiments show that surface sites into the channels have a low accessibility to bulk molecules, and the diameter of these channels (inferior to 4 Å) probably induces a steric hindrance in the case of pyridine molecules. So, at least for pyridine, the detected Lewis acid sites probably characterize only some defects localized onto the outer surface of the crystallites. Theses defects are certainly associated to the presence of M^{3+} coordinatively unsaturated (cus) ions with coordinative vacancies due to fluorine departure. On γ-Al_2O_3, two ν_{8a} bands of coordinated pyridine and 3 $\delta_s(NH_3)$ bands of coordinated ammonia have been reported, assigned to different configurations of surface cus Al^{3+}, as expected by the presence of both $_{tetra}Al^{3+}$ and $_{octa}Al^{3+}$ in the spinel structure.[27,30] The observation of only one ν_{8a} pyridine band and one $\delta_s(NH_3)$ band in the spectra related to $AlF_{3-x}(OH)_x$ suggests the presence of only one type of cus Al^{3+} cations on its surface. On α-alumina samples, where from structural considerations Al^{3+} cations in octahedral position are only expected, it has been reported that the Lewis acidity of such coordinatively unsaturated cations is very low, as shown by pyridine adsorption giving rise to a ν_{8a} band at a wavenumber lower than 1600 cm^{-1}.[31] In a recent paper devoted to the acidity of α-gallia (a compound expected to also present only cations in octahedral position), it has been however reported that surface reconstruction occurs, leading to surface cations in tetrahedral position, explaining the high surface Lewis acidity of α-gallia.[32] The same phenomenon could occur in the case of $AlF_{3-x}(OH)_x$; ^{27}Al NMR studies are planned to check such a hypothesis.

The size of the NH_3 molecule is close to that of water. So, NH_3 probes the acidic sites on the outer surface and those into the channels, the latter containing the hydroxyls exchangeable by D_2O. Moreover, on the surface, the protonation of ammonia is generally easier than that of pyridine and therefore NH_3 can probe weaker acidic sites on oxide surfaces.[27] Coordinated NH_3 gives rise to the two bands situated near 1300 ($\delta_s(NH_3)$) and 1610 cm^{-1} ($\delta_a(NH_3)$). Datka et al. in a study devoted to zeolites[33] determined the apparent molar extinction coefficient of the band near 1610 cm^{-1} (0,022 cm^2 μmol^{-1}). Extending it to HTB materials, and taking into account the intensity of the 1610 cm^{-1} band, a total number of NH_3 coordinated species of about 300 and 450 μmol g^{-1} can be estimated for $FeF_{3-x}(OH)_x$ and $Fe_{0.8}Cr_{0.2}F_{3-x}(OH)_x$, respectively. Though not very accurate due the weakness of the intensity of the $\delta_a(NH_3)$ band, such values are much higher than those determined from pyridine adsorption (100−125 μmol g^{-1}). This strongly suggests the presence of Lewis acid sites in the channels of the HTB materials considered. This could be related to the relatively high temperature used to activate these samples, a temperature close to that for which fluorine departure has been evidenced.[13]

Except for $FeF_{3-x}(OH)_x$, no pyridinium species have been detected on the materials studied. Moreover, under 133 Pa of pyridine at equilibrium pressure, no band at about 1595 cm^{-1} characterizing H-bonded species has been observed. We conclude that the detection of Brønsted acid sites by NH_3 only is not due to its different basicity respect to pyridine but to its

smaller size, allowing us to situate these sites only in the channels. The sharpness of the 1425 cm^{-1} band and the absence of the corresponding $\delta_a(NH_4)$ one near 1680 cm^{-1} show that the NH_4 species formed have a high symmetry and that the sites are homogeneous. Curves reported in Figure 8 show a linear decrease of the $\nu+\delta$(OH) band intensity versus the amount of ammonia introduced. This unambiguously evidences that OH groups in the channels participate to ammonium formation.

Note that on $CrF_{3-x}(OH)_x$ no pyridinium formation is observed and only a weak pyridinium signal is detected on $FeF_{3-x}(OH)_x$, easily eliminated by evacuation. So, the larger part of Brønsted acidic sites is probably localized inside the channels and only perturbed by ammonia.

On corresponding metal oxides, ammonium bands are not detected onto the surface of hematite after NH_3 adsorption.[18] This absence of strong Brønsted acidic sites on iron oxide is confirmed by pyridine adsorption on α- and γ-Fe_2O_3:[28,18] no pyridinium species are reported, only coordinated and H-bonded species are evidenced. On α-Cr_2O_3, Brønsted acidity of OH groups probed by CO has been studied by Knözinger:[19] the perturbation of hydroxy groups by CO adsorption at low temperature is very weak ($\Delta\nu$(OH) < 75 cm^{-1}), thus showing the absence of strong Brønsted acid sites. So, stronger Brønsted acidity of HTB materials is observed compared to that of metal oxides containing the same metal. This phenomenon can be explained involving the high electronegativity of fluorine, leading to the strengthening of the M−OH bond corresponding to adjacent hydroxyls and to the weakening of the O−H bond. This fluorine effect is often invoked to explain the creation of strong Brønsted sites on alumina after fluorination.[1]

From a quantitative point of view, we have evaluated the density of Brønsted acid sites by calculating the amount of ammonium species formed after ammonia introduction on $FeF_{3-x}(OH)_x$ and $Fe_{0.8}Cr_{0.2}F_{3-x}(OH)_x$ compounds. Assuming that one ammonium species corresponds to one hydroxy group (that is realistic, considering the narrowness of the channels), and taking into account that we have 12 cations per unit cell, we deduce that 1.8 and 1 OH groups per unit cell are awaited, respectively.

However, the following observation strongly suggests that hydroxyls are not the sole Brønsted acid sites interacting with ammonia: during ammonia evacuation at room temperature and up to 473 K, the decrease of the ammonium bands intensity at about 3200 and 1425 cm^{-1} is observed (Figure 8) while no ν-(OH) bands are clearly restored (spectra 1h, 1g, 2h, 2i, and 2j, Figure 6). This shows that some protonated species desorb at low temperature and do not involve hydroxy groups. Clet et al. reported on chlorinated alumina the presence of protonated species after pyridine or lutidine adsorption, easily desorbed by vacuum at low temperature.[34] They suggest that Brønsted sites are not necessarily weakly acid and explain the phenomenon by the presence of HCl loosely bound onto the surface, giving rise to labile Cl-pyH^+ species. In the present case, we propose as the origin of these easily desorbed ammonium species F−NH_4^+ complex formation due to some residual presence of chemisorbed HF molecules onto the surface. Such HF species could be either in pores (easiness of NH_4 desorption) or on the surface of $FeF_{3-x}(OH)_x$, since pyridinium species formation does not apparently involve hydroxyls.

Conclusions

Thanks to the presence of hydroxy groups as "impurities" substituting fluorine into the samples, infrared spectroscopy appears a suitable method to study the acid properties of HTB fluorinated materials. Using basic probes with different sizes (pyridine and ammonia), it was possible to determine the localization of Brønsted and Lewis acid sites, their strength in the case of Lewis acidity, and their amount. To specify the strength of hydroxy group Brønsted acidity in the channels, experiments using CO adsorption at low temperature are planned.

The catalytic activity studies of these materials for synthesis of CFCs and HFCs molecules show that the Lewis acid sites seem to be the active sites, whereas the presence of Brønsted acid sites hinders the reaction. Therefore, the formation of OH groups should be avoided in such compounds. By contrast, it is well-known that fluorinated materials are better catalysts than metal oxides for hydrocarbon conversion due to the presence of strong Brønsted acid sites, suggesting the promoting effect of hydroxyls in the latter case. So another important point is the determination of the role and the accessibility of OH groups in HTB fluorinated compounds for catalyst experiments by adjusting the F^-/OH^- ratio by water addition. IR spectroscopy appears to be a powerful technique for these kinds of studies.

Acknowledgment. This work has been supported by Rhodia Recherches (Centre de Recherches d'Aubervilliers, France).

References and Notes

(1) Ghost, A. K.; Kydd, R. A. *Catal. Rev. Sci. Eng.* **1985**, *27*, 539.
(2) Rodriguez, L. M.; Alcaraz, J.; Hernandez, M.; Dufaux, M.; Ben Taârit, Y.; Vrinat, M. *Appl. Catal. A: General* **1999**, *189*, 53.
(3) Kemnitz, E.; Menz, D.-H. *Prog. Solid State Chem.* **1998**, *26*, 97.
(4) Badri, A.; Binet, C.; Lavalley, J.-C. *J. Chem. Soc., Faraday Trans.* **1997**, *93*, 2121.
(5) Kerkhov, F. P. J. M.; Oudejans, J. C.; Moulijn, J. A.; Matulewicz, E. R. A. *J. Colloid Interface Sci.* **1980**, *120*, 77.
(6) Scokart, P. O.; Selim, S. A.; Damon, J. P.; Rouxhet, P. G. *J. Colloid Interface Sci.* **1979**, *70*, 209.
(7) Le Bail, A.; Jacoboni, C.; Leblanc, M.; de Pape, R.; Duroy, H.; Fourquet, J. L. *J. Solid State Chem.* **1988**, *77*, 96.
(8) Leblanc, M.; Ferey, G.; Chevalier, P.; Calage, Y.; de Pape, R. *J. Solid State Chem.* **1983**, *47*, 53.
(9) Francke, L.; Durand, E.; Demourgues, A.; Vimont, A.; Daturi, M.; Tressaud, A. *J. Mater. Chem.* **2003**, *13*, 2330.
(10) Hess, A.; Kemnitz, E. *J. Catal*. **1994**, *149*, 449.
(11) Morterra, C.; Cerrato, G.; Cuzzato, P.; Masiero, A.; Padovan, M. *J. Chem. Soc., Faraday. Trans.* **1992**, *88*, 2239.
(12) Kemnitz, E.; Hess, A.; Rother, G.; Troyanov, S. *J. Catal.* **1996**, *159*, 332.
(13) Demourgues, A.; Francke, L.; Durand, E.; Tressaud, A. *J. Fluorine Chem.* **2002**, *114*, 229.
(14) Khabtou, S.; Chevreau, T.; Lavalley, J.-C. *Micro. Mater.* **1994**, *3*, 133.
(15) Morterra, C.; Chiorino, A.; Ghiotti, G.; Garrone, E. *J. Chem. Soc., Faraday. Trans.* **1979**, *75*, 27.
(16) Davydov, A. A. In *Infrared spectroscopy of adsorbed species on the surface of transition metal oxides*; Rochester, C. H., Ed.; J. Wiley & Sons Ltd.: New York, 1990.
(17) Saussey, J. Private communication
(18) Lorenzelli, V.; Busca, G. *Mater. Chem. Phys.* **1985**, *13*, 201.
(19) Zaki, M. I.; Knözinger, H. *Mater. Chem. Phys.* **1987**, *17*, 201.
(20) Jacobs, P. A.; Nortier, W. J. *Zeolites* **1982**, *2*, 226.
(21) Tsyganenko, A. A.; Lamotte, J.; Saussey, J.; Lavalley J.-C. *J. Chem. Soc., Faraday Trans. 1.* **1989**, *85*, 2397
(22) Lavalley, J.-C.; Bensitel, M.; Gallas, J.-P.; Lamotte, J.; Busca, G.; Lorenzelli, V. *J. Mol. Struct.* **1988**, *175*, 453.
(23) Burneau, A.; Gallas, J.-P. In *The surface properties of silicas*; Legrand, A. P., Ed.; J. Wiley & Sons Ltd.: New York, 1998; Chapter 3A.
(24) Ishikawa, T.; Cai, W. Y.; Kandori, K. *J. Chem. Soc., Faraday Trans* **1992**, *88*, 1173.
(25) Mariette, L.; Hemidy, J.-F.; Cornet, D. *Stud. Surf. Sci.* **1985**, *21*, 263; Che, M., Bond, G. C, Eds.
(26) Kustov, L. M.; Borovkov, V. Y.; Kazansky, V. B. *J. Catal*. **1981**, *72*, 149.
(27) Busca, G. *Phys. Chem. Chem. Phys.* **1999**, *1*, 723.

(28) Harrouche, N.; Batis, H.; Ghorbel, A. *J. Chim. Phys.* **1984**, *81*, 267.

(29) Zecchina, A.; Coluccia, E.; Guglielminotti, S.; Ghiotti, G. *J. Phys. Chem.* **1971**, *75*, 2774.

(30) Morterra, C.; Chiorino, A.; Ghiotti, G., Garrone, E. *J. Chem. Soc., Faraday Trans. 1* **1979**, *75*, 271.

(31) Morterra, C.; Magnacca, G. *Catal. Today* **1996**, *27*, 497.

(32) Lavalley, C.; Daturi, M.; Montouillout, V.; Clet, G.; Otero Arean, C.; Rodriguez Delgado, M.; Sahibed-dine, A. *Phys. Chem. Chem. Phys.* **2003**, *5*, 1301.

(33) Datka, J.; Gil, B.; Kubacka, A. *Zeolites* **1995,** *15*, 501

(34) Clet, G.; Goupil, J.-M.; Cornet, D. *Bull. Soc. Chim. Fr.* **1997**, *134*, 223.